Tunneling density of states as a function of thickness in superconductor/strong ferromagnet bilayers

S. Reymond,[1] P. SanGiorgio,[2,*] M. R. Beasley,[1] J. Kim,[3] T. Kim,[3] and K. Char[3]
[1]*Department of Applied Physics, Stanford University, Stanford, California 94305, USA*
[2]*Department of Physics, Stanford University, Stanford, California 94305, USA*
[3]*Center for Strongly Correlated Materials Research, School of Physics, Seoul National University, Seoul 151-742, Korea*
(Received 10 June 2005; revised manuscript received 3 January 2006; published 13 February 2006)

We have made an experimental study of the tunneling density of states (DOS) in strong ferromagnetic thin films (CoFe) in proximity with a thick superconducting film (Nb) as a function of the ferromagnetic thickness d_F. Remarkably, we find that as d_F increases, the superconducting DOS exhibits a scaling behavior in which the deviations from the normal-state conductance have a universal shape, which decreases exponentially in amplitude. The decay length d_1 is approximately 0.4 nm. We do not see oscillations in the DOS as a function of d_F, as one would expect from predictions based on the Usadel equations using reasonable parameters.

DOI: 10.1103/PhysRevB.73.054505 PACS number(s): 74.45.+c, 73.40.Gk

I. INTRODUCTION

One of the incompletely solved problems in conventional (noncuprate) superconductivity is the interaction between superconductivity and magnetism. This issue arises most prominently in the context of the so-called magnet superconductors (e.g., $CeCoIn_5$) and in the superconductor/ferromagnet (SF) proximity effect. One striking effect expected for a superconductor in the presence of an exchange field is the existence of spatial modulations of the superconducting pair wave function (see, for instance, Ref. 1). These oscillations occur in a new superconducting state where the center of mass of pairs acquires a nonzero momentum. This state was predicted 40 years ago and is known as the Fulde-Ferrell-Larkin-Ovchinnikov (FFLO) state.[2,3] In the case of the SF proximity effect, this oscillating pair wave function is expected to exponentially decay into the F layer. These oscillations, in turn, are predicted to lead to oscillations in the critical temperature of SF bilayers,[4,5] inversions of the density of states (DOS),[6,7] and changes in the sign of the Josephson coupling in SFS sandwiches[8] (creating a so-called π junction), as the F layer thickness d_F is varied. Even more exotic predictions include possible odd-frequency triplet superconductivity.[9]

Indeed, a vast theoretical literature now exists regarding the SF proximity effect (for a thorough review, see Ref. 10), mostly concerning systems with a uniform magnetization in the F layer (which assumes a single-band model with an exchange field, $E_{ex} \ll E_F$) in the dirty quasiclassical limit (i.e., where all the characteristic lengths are larger than both λ_F, the Fermi wavelength, and ℓ, the mean free path). In this situation, the superconducting properties can be calculated using the Usadel equation.[11] Still, explicit predictions may differ depending on the importance of scattering processes[1] or on the boundary conditions, which can be resistive[5] or magnetically active.[12]

Experimentally, phase sensitive measurements in some SFS structures clearly demonstrate the existence of π junctions.[13–15] On the other hand, critical temperature measurements in SF structures have shown a variety of behaviors as a function of d_F. Everything from monotonic dependence to steplike features, small dips, and oscillations have been reported.[5,16–19] It has been pointed out that important parameters such as the size of the exchange field E_{ex} and the boundary resistance γ_b can evolve naturally as a function of d_F.[20] What makes these results particularly hard to interpret is that all of these changes typically take place within a few nanometers, just like the expected oscillation of the superconducting wave function inside the F material.

Previous tunneling measurements have also produced mixed results. A clear inversion in the DOS as a function of d_F was reported in planar tunneling junctions composed of niobium and the weakly ferromagnetic alloy PdNi,[21,22] yet STM studies on very similar Nb/CuNi bilayers did not show a repeatable inversion in the DOS.[23,24] A study of strongly ferromagnetic layers was performed on the superconducting side of Pb/Ni bilayers and no indication of oscillatory behavior was seen.[25]

In this paper we present density of state spectroscopy studies using tunneling junction located on the F side of $Nb/Co_{0.6}Fe_{0.4}$ bilayers. CoFe is a strong ferromagnet with a Curie temperature of approximately 1200 K widely used in magnetic tunnel junction devices due to the high quality of the interface it makes with aluminum oxide, which is now the standard choice for tunneling barriers. Based on low-temperature resistivity, we estimate the diffusion constant in CoFe, D, to be 1.4×10^{-3} m^2 s^{-1} and the mean free path ℓ to be 1.0 nm. The critical temperatures of similarly deposited Nb/CoFe bilayers are shown in Fig. 1. Here, a slight dip at $d_F = 2$ nm is noticeable before saturation at large d_F. A quantitative analysis of these data based on the Usadel equations[26] gave a value of 100 meV for the exchange field E_{ex} and 0.34 for the interface resistance parameter γ_b which is fairly transparent. In these samples, though, a thin Nb layer (18 nm) was deposited first, and then the CoFe was deposited on top. They differ from our junctions which have a thicker Nb layer (50 nm) deposited on top of a thin CoFe layer. Thus the SF interface are not rigorously identical. Regardless of these details, we still expect that any inversion in the DOS that may arise in our samples would occur at

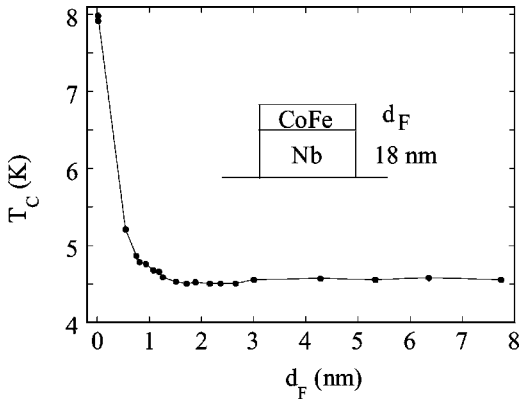

FIG. 1. T_c as a function of CoFe thickness in Nb/CoFe thin films with $d_{Nb}=18$ nm, the error bars are smaller than the plotted points. A minimum is repeatedly found at $d_{CoFe}=2$ nm. Fitting the data with the Usadel equation gives $\gamma_b=0.34$, $E_{ex}=0.1$ mV, $D=1.4\times10^{-3}$ m^2 s^{-1}, and $\xi_F=1$ nm, in the standard notation.

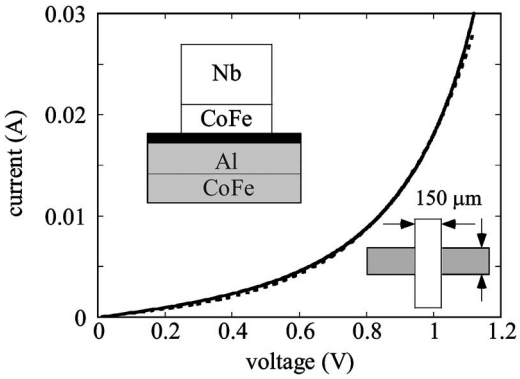

FIG. 2. I-V of a typical Al/AlO_x/Nb junction taken at 10 K (solid) and the theoretical fit (dashed line) with Eq. (1). The fitting parameters are: $\phi=1.74$ eV, $t=1.69$ nm, and $A=132^2$ nm^2. We found similar parameters for all other junctions. Left inset: sample top view. Right inset: junction cross section. The black area represent the AlO_x layer.

roughly the same thickness as the dip in T_c, which is between 1 and 2 nm. In other words, we expect $\xi_F=\sqrt{\hbar D/2E_{ex}}\approx1$ nm. Thus we performed tunneling spectroscopy on samples with thicknesses ranging from 0 to 4.5 nm in increments of 0.5 nm.

II. SAMPLE PREPARATION

Our junctions are deposited and patterned entirely *in situ* in a dc magnetron sputtering system, described here.[26] The geometry of the tunneling structures is pictured in the inset of Fig. 3. A thin (3 nm) CoFe layer is deposited below the Al layer, in order to suppress superconductivity in the counterelectrode. As a result the Al layer remains normal down to the lowest measured temperatures. An atomic oxygen source is used to oxidize the Al to a thickness of ≈2 nm. The stencil mask is then changed and without breaking vacuum a CoFe layer and then a Nb layer are immediately deposited. To establish a robust superconducting state in the S layer, we deposit approximately 50 nm of Nb, which is sufficiently thick to ensure that there were only small changes in $T_c(d_F)$. However, the Nb thickness was not tightly controlled and consequently our samples display a small but nonsystematic spread in T_c. Typical junction resistances are roughly 200 Ω at room temperature (about 1.2 times greater at 10 K), with a trend to higher junction resistances with increased CoFe thickness.

To characterize the quality of our tunnel junctions, we compare I-V curves taken slightly above T_c with a simple tunneling model, following the standard approach of Ref. 27. Here, the electrodes are idealized as Fermi gases with equal Fermi energies μ of 12 eV. The oxide layer is modeled as a finite barrier with height ϕ and thickness t. At $T=0$, the only other free parameter is the junction area A. Using the WKB approximation to calculate the probability of transmission when a potential V is applied across the electrodes, the current is given by

$$I(V)=A\frac{4\pi me}{h^3}\int_{\mu-eV}^{\mu}e^{-2t(2m/\hbar^2)^{1/2}(\phi+\mu-eV/2-E)^{1/2}}EdE, \tag{1}$$

where m is the mass of the electron. Although this model neglects the difference in Fermi energy between the two metals, distortions of the barrier, and other details, we find that it accurately fits our data with very reasonable parameters. A characteristic fit for an Al/AlO_x/Nb junction is shown in Fig. 2. Similar analyses were performed on Al/AlO_x/CoFe/Nb junctions. In all cases, we find that $\phi=1.7$ eV, $t=1.7$ nm, and $A=130^2$ nm^2, which corresponds well to the actual junction area, 150^2 nm^2.

III. RESULTS

Tunneling measurements shown below are taken at 0.3 K using standard lock-in techniques to measure the differential resistance; variations as small as few parts in 10 000 could be measured. This resolution allows us to distinguish small features in the tunneling spectrum, which is the key to measure proximity structures where superconductivity can be strongly attenuated.

Junctions grown without the ferromagnetic layer show a clean superconducting DOS spectrum (see the bottom curve of Fig. 4). In Al/AlO_x/Nb, the zero-bias conductance (ZBC) is 0.04 times the normal conductance. The spectrum can be well fitted by a BCS spectrum at 0.3 K, yielding an energy gap Δ of 1.35 meV. We have checked that the DOS remains unchanged when a 5-nm-thick gold layer is inserted between the Nb and the tunneling barrier (the structure is then Al/AlO_x/Au/Nb).

The DOS is dramatically different when a CoFe layer is inserted instead of the normal metal: the superconducting signals becomes very weak—a few percent of the normal conductance when $d_F=1$ nm and less than a part per thousand when $d_F=3$ nm. It is therefore crucial to be able to separate the superconducting component from the normal

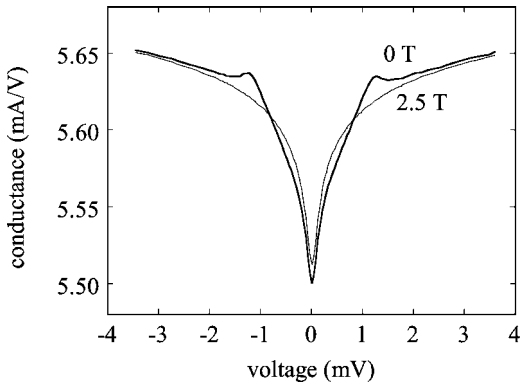

FIG. 3. Raw conductance data taken at 0.5 K in a Nb/CoFe/AlO_x/Al/CoFe junction at zero field (thick line) and above the Nb critical field (thin line). Here d_F=2.5 nm.

DOS. This is possible using in-field measurement. Figure 3 shows typical conductance spectra taken in zero field (thick line) and with a perpendicular magnetic field of 2.5 T (thin line), just above the critical field H_{c2}. The zero-field curve clearly reveals superconducting contributions to the density of states, but they are superposed on top of a nonconstant background conductance. The high-field data show this background conductance, which is in general a V-shaped curve, centered at zero volts, with the conductance at 1 mV typically 2% larger than the zero-bias conductance. The main difficulty lies in extracting the superconducting DOS from this background. For our "thicker" samples ($d_F > 1$ nm), we find that the background conductance, although temperature dependant, was not affected by either the magnitude or orientation of the applied magnetic field. Thus we simply divide the zero-field curve by the in-field curve to isolate the superconducting signal. But for samples with thin CoFe layers (less than 1.5 nm), above H_{c2} and at low temperatures (below roughly 3 K), we see a zero-bias conductance dip, which increased in depth linearly with increasing field, similar to previous studies.[28] For these samples, the zero-field normal-state background could only be calculated by studying the field-dependence of this feature and extrapolating it to zero field. In any event, for these samples the superconducting features were large enough that the end result was insensitive to the details of the normalization.

Figure 4 shows the resulting curves for all measured thicknesses. Note that in the top panel the scale is amplified about a thousand times. Beginning at the bottom of the figure, we see the clean DOS curve of the Nb. When the thinnest (0.5 nm) F layer is added to the superconductor, the BCS-like tunneling spectrum is abruptly altered with substantial conductance below the gap energy. As d_F increases further, the superconducting features in the tunneling conductance are strongly attenuated. Above 2.0 nm, a narrow zero-bias conductance peak develops which is suppressed in fields greater than H_{c2}; this suggests it is either related to superconductivity, or a remnant of our normalization procedure, but due to its weak signal-to-noise ratio, we do not focus on it in the present discussion. When d_F exceeds 3.5 nm, all recognizable features disappear and the normalized conductance is equal to 1 ± 10^{-4}.

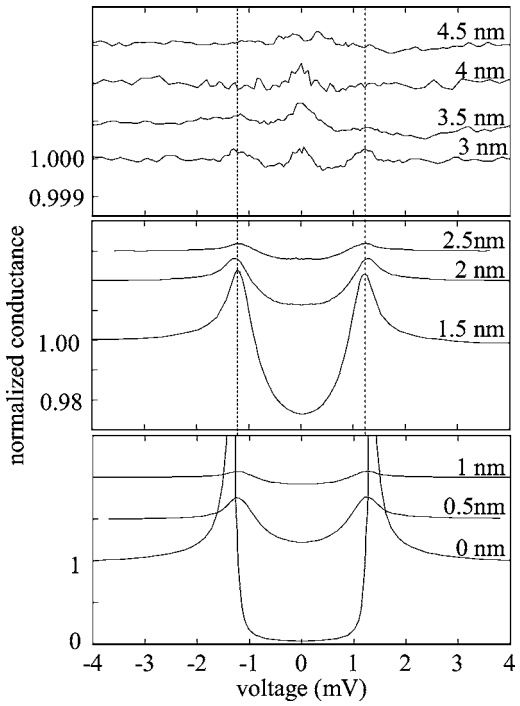

FIG. 4. Normalized conductances taken at 0.3 K for various CoFe thickness indicated inside. From the bottom to the top plot the vertical scale is successively amplified. The curves are shifted for clarity. The dashed line shows that the peaks energy remains unchanged from 0.5 to 3 nm.

The most striking observation, though, is that between 0.5 and 2.5 nm the spectra can be rescaled onto a single curve. That is to say,

$$\sigma(V,d_F) - 1 = A(d_F)[N(V) - 1], \tag{2}$$

where $N(V)$ is a generic, thickness independent function and $A(d_F)$ is a scaling coefficient. The curves, rescaled so that the zero-bias conductance vanishes, are shown in Fig. 5. Their overlap demonstrates well the generic nature of $N(V)$. $A(d_F)$, defined so that $N(0)=0$, is plotted in Fig. 6 (full circles). The straight line is an exponential fit of the data, which suggests that our scaling coefficient is given by

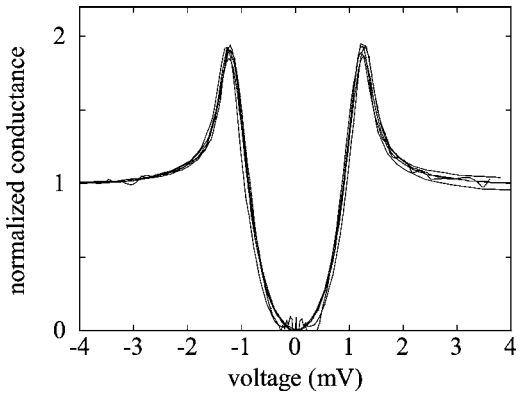

FIG. 5. Superposition of five scaled conductance curves for d_F =0.5–2.5 nm. The d_F=2.5-nm curve is scaled by a factor of 500.

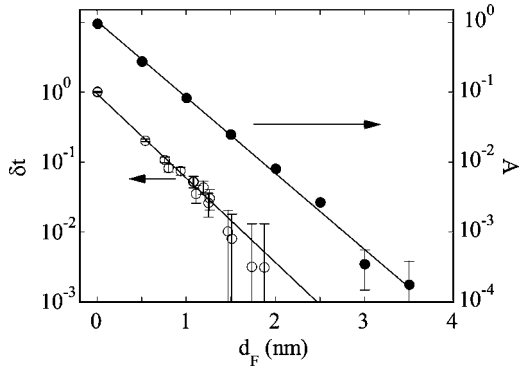

FIG. 6. Scaling factor, $A(d_F)=1-\mathrm{ZBC}$, and normalized transition temperature, $\delta t=(T_c-\mathrm{Min}[T_c])/T_c(d_F=0)$. Only the initial decay of δt is plotted ($d_F<2$ nm). The dotted line is an attempt to fit $A(d_F)$ with Eq. (7). The parameters used for the fit are $\Delta=1.35$ meV, $T=0.3$ K, $\Gamma_{AG}=360$ meV, and $E_{ex}=155$ meV.

$$A(d_F) = e^{-d_F/d_1}, \tag{3}$$

where $d_1=0.4$ nm. Since $A(d_F\to 0)=1$, $N(V)$ can be interpreted as the tunneling DOS inside F as $d_F\to 0$. The remarkable fact that $A(d_F)$ extrapolates to 1 as d_F tends to zero is not required by the scaling procedure. It offers more evidence that the interface between the Nb and CoFe layer is fairly transparent, as a large boundary resistance would increase the zero-bias conductance discontinuously at $d_F=0$. Note also that the zero-bias conductance is simply $1-A(d_F)$ and therefore rises exponentially from zero as d_F increases.

An important characteristic of the generic DOS $N(V)$ is that the sum rule on the DOS is satisfied within 1%. This not only justifies the procedure used to extract the superconducting DOS, it also suggests that the tunneling barrier is not weakened by the addition of the CoFe layer. A weakening would result in an excess current within the gap, raising the total spectral area above unity.[29]

Comparing these tunneling data with the T_c measurements shown in Fig. 1, we see that, like the attenuation of the DOS, the initial drop of T_c follows an exponential decay with a characteristic length, $d_1=0.4$ nm. To make this obvious, we plot in Fig. 6 the normalized critical temperature, $\delta t=(T_c-\mathrm{Min}[T_c])/T_c(d_F=0)$, together with the scaling factor $A(d_F)$. The similarity between the two measurements indicates that, even though the deposition order is reversed, the interface is likely to be similar in both types of sample. However, our tunneling measurements, probing directly the pair wave function *inside the F material*, do not confirm the existence of an oscillation between 0 and 3.5 nm, as suggested by the shallow dip of T_c around 2 nm.

IV. DISCUSSION

Since it is commonly used to describe hybrid superconducting systems, we examine here if the Usadel equation can satisfactorily describe the proximity effect in our films. For this purpose, we assume that the approximations needed are valid, namely that our system is in the diffusive quasiclassical limit, even though both $\ell=1.0$ nm and the Fermi wavelength (about 0.5 nm) are not much smaller than d_1. Since we do not observe oscillations in the proximity region, it is clear that the usual Usadel equation[1,5] does not describe our data. Nevertheless, others[22,24] have included an Abrikosov-Gorkov pair-breaking term in the Usadel equation, which can diminish or even eliminate oscillations. In this context, the equation in the F materials reads

$$-\frac{\hbar D}{2}\frac{d^2\Theta}{dx^2} + (\omega + iE_{ex})\sin\Theta + 2\Gamma_{AG}\sin\Theta\cos\Theta = 0, \tag{4}$$

where $\sin\Theta$ and $\cos\Theta$ are the superfluid and normal electron densities, respectively, and Γ_{AG} is the Abrikosov-Gorkov pair-breaking rate, in the notation of Ref. 22, which is equal to $1/2\tau_s$, the magnetic scattering time, in the notation of Ref. 24. If we linearize Eq. (4) for small Θ, we immediately see that solutions will be of the form

$$\Theta \propto e^{-k_r x - ik_i x}, \tag{5}$$

where k_r and k_i characterize the exponential decay and oscillatory behavior, respectively. Since the DOS is given by $\mathrm{Re}\{\cos[\Theta(d_F,\omega\to iE)]\}\approx\mathrm{Re}[1-\Theta^2/2]$, the exponential decay length of the ZBC, d_1, will be $(2k_r)^{-1}$ and the distance at which the DOS becomes inverted, which we will call d_2, will be roughly $\pi/4k_i$. If we solve for E_{ex} and Γ_{AG} in terms of d_1 and d_2, we get

$$E_{ex}=\frac{\pi\hbar D}{8d_1d_2};\quad \Gamma_{AG}=\frac{\hbar D}{4}\left(\frac{1}{(2d_1)^2}-\frac{\pi^2}{(4d_2)^2}\right). \tag{6}$$

From our data, we have that $d_1=0.4$ nm. Since we see no inversion in the DOS data, d_2 must be greater than at least 3.0 nm, i.e., $d_2\gg d_1$. Using these values, it follows directly that $\Gamma_{AG}=360$ meV and $E_{ex}<300$ meV. The limit on E_{ex} is consistent with estimates of E_{ex} from measurements on bulk samples using the relation $E_{ex}=(3/2)k_BT_C$, which for $T_C=1200$ K yields $E_{ex}=155$ meV.[30,31] Taking the bulk value is reasonable because previous studies have shown nearly bulk ferromagnetic ordering present in films of CoFe as thin as 1 nm.[32] In addition, the clean exponential decay as a function of d_F up to 3.5 nm seems incompatible with any variation of material parameters from sample to sample, therefore E_{ex} is most likely equal to the bulk value in every sample. Taking the measured d_1 and $E_{ex}=155$ meV, one can fix the value $d_2=5.9$ nm. With these values, we find that $\xi_F=1.7$ nm and the spin-relaxation length $L_s=\sqrt{\hbar D/2\Gamma_{AG}}=1.1$ nm.

Using the above estimates of E_{ex} and Γ_{AG}, it is possible to test for self-consistency within the Usadel theory by calculating the predicted zero-bias current (ZBC) and density of states. If we impose the boundary condition that $\Theta=\Theta_{BCS}$ at the interface with the superconductor ($x=0$), which is a reasonable simplification for a transparent interface, and that $d\Theta/dx=0$ at the interface with the oxide layer ($x=d_F$), we can solve for $\mathrm{Re}[\cos\Theta(d_F)]$, the tunneling DOS as a function of energy, $E=-i\omega$. An approximate solution to the complete nonlinear system is derived in Ref. 24, which we adapt with only minor notational changes,

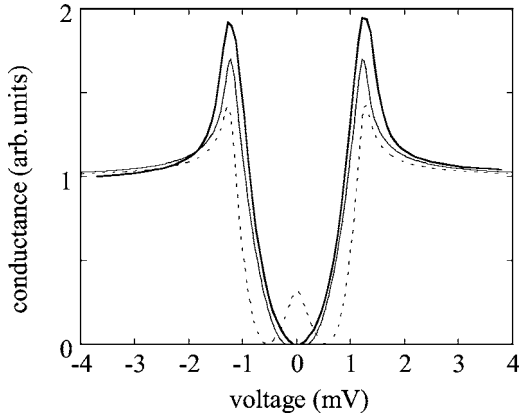

FIG. 7. Comparison of scaled experimental results (thick line) with predictions of Eq. (7), with $E_{ex}=155$ meV (dotted line) and $E_{ex}=36$ meV (thin line).

$$\Theta = \frac{8}{\sqrt{1-p^2}} \exp(-\sqrt{i+\tilde{\gamma}+i\tilde{\omega}\tilde{x}}) \times \sqrt{\frac{\sqrt{1-p^2\sin^2\frac{\Theta_0}{2}}-\cos\frac{\Theta_0}{2}}{\sqrt{1-p^2\sin^2\frac{\Theta_0}{2}}+\cos\frac{\Theta_0}{2}}}, \quad (7)$$

where $\tilde{\gamma}=2\Gamma_{AG}/E_{ex}$, $\tilde{\omega}=E/E_{ex}$, $\tilde{x}=x/\xi_F$, $p^2=(1+i/\tilde{\gamma})^{-1}$, and $\cos\Theta_0=\cos\Theta_{BCS}=|E|/\sqrt{E^2-\Delta^2}$.

The predicted ZBC of our tunnel junctions is given by $\mathrm{Re}[\cos\Theta(d_F,E=0)]$, which is plotted in Fig. 6 for $\Gamma_{AG}=360$ meV and $E_{ex}=155$ meV (dotted line). As expected, the slope of the theoretical fit and the experimental data matches well, but the theoretical fit is offset from the experimental data by roughly 0.8 nm. Thus it is clear that this application of the linearized theory is inconsistent with our tunneling data, even in the limit of large d_F. At this time, one might be tempted to try to improve the fit by adding an effective thickness, thickness-dependent parameters, or possibly a large boundary resistance, but we find no physical justification for this added complication. As noted above, the clear exponential decay of our ZBC coupled with the constant shape of our conductance curves argues against a strong thickness dependence of either Γ_{AG} or E_{ex} and the extrapolation of our ZBC to zero as $d_F\rightarrow 0$ argues against a large boundary resistance. Thus we conclude that the linearized Usadel equation does not describe our data well at all.

Still, since our conductance spectra all have the same shape, independent of scale, it is interesting to compare this shape with the linearized Usadel theory spectra. As noted here,[22] for $d_F \gg \xi_F$, the predicted spectra will also display scaling behavior. Thus we can calculate the conductance for a sufficiently large d_F and then scale it appropriately to compare with our data. The results of this procedure are displayed in Fig. 7. The dashed line is the calculated and scaled spectrum for $\Gamma_{AG}=360$ meV and $E_{ex}=155$ meV, while the solid line is calculated for $\Gamma_{AG}=360$ meV and $E_{ex}=36$ meV. Clearly, the curve with the bulk exchange field, 155 meV, does not fit our generic shape, whereas the curve with the much smaller exchange field, 36 meV, compares well with our data.

Now, we must consider whether the fitting parameters used above are physically meaningful. First, we note that we are only able to match the shape of our conductance curves by using a very small E_{ex}. Previous tunneling measurements have also reported this effect;[21,22,24] they suggest that either the nearby superconductor is suppressing the ferromagnetic ordering, or that it is not fully established in such thin films. Both of these are highly plausible given the low Curie temperature of the magnetic alloys used, but we find these possibilities to be less compelling when describing the magnetic properties of CoFe, which should be much more strongly ordered. Further, we find that conductance spectra taken at zero field showed no change after either a large parallel or perpendicular magnetic field was applied, suggesting that domain size and structure to not affect our results. All of this suggests that the magnetic properties of our samples, namely E_{ex}, is fairly constant as a function of thickness and therefore equal to the bulk value of 160 meV. Thus we consider the value suggested by the linearized Usadel analysis ($E_{ex}=36$ meV) to be unphysical.

Since Γ_{AG} is related to the spin-dependent scattering length L_s, it too has been studied in the context of GMR. As mentioned above, our value of Γ_{AG} corresponds to $L_s=1.1$ nm. This is considerably smaller than the value determined by GMR effects, which for a slightly different alloy ($Co_{91}Fe_9$) was found to be 12 ± 1 nm at low temperature,[33] which corresponds to roughly 3 meV. This value seems much more reasonable than ours, since it corresponds to a spin-scattering energy which is much smaller than the exchange field—a necessary condition for ferromagnetism to occur in a single-band model. Thus, as with E_{ex}, we find that the value suggested by the linearized Usadel analysis ($\Gamma_{AG}=360$ meV) is unreasonable.

One final prospect is that a strong exchange field exists, but that the oscillations it would induce in the DOS are washed out by lateral variations in the thicknesses of the samples.[34] We note that these variations would have to be very large ($\delta d_F \sim d_1$), and that we did not see any sample-to-sample variation for the same d_F. Finally, we note that the Usadel equation is only strictly valid in the diffusive limit, wherein all relevant length scales are larger than the mean free path ℓ. Although ξ_F and L_s calculated above are greater than $\ell=1$ nm, our thinnest SF sample has $d_F=0.5$ nm, which is not. Thus one strong possibility is that in going from the more general Eilenberger equations[35] to the diffusive Usadel equations, the effect of the exchange field is being lost or possibly recast as an effective Γ_{AG}. However, even if the Usadel equation does not apply to our system, the predicted action of an exchange field on the superconducting wave function should hold. Indeed we do see a dramatic pair-breaking effect, but no evidence of the FFLO state. In light of the totality of the considerations above, we come to the position that no reasonable application of the conventional Usadel theory or purely materials problem can account for our results.

V. CONCLUSION

In summary, we have measured the tunneling DOS on the F side of SF bilayers and have found a sharp change in the shape of the conductance curves between $d_F=0$ and $d_F=0.5$ nm and that for all $d_F>0$, the shape of the conductance curves is universal. The only dependence on d_F is given by an exponential decrease in the magnitude of the superconducting signal with characteristic length $d_1=0.4$ nm. We also note a similar exponential decrease in $T_c(d_F)$ in related samples. Finally, we note that we have been unable to reconcile our results with a conventional application of the Usadel equation.

ACKNOWLEDGMENTS

We thank L. Litvak and Y. Bazaliy for stimulating discussions. We also thank T. Kontos and O. Valls for helpful communications. The authors acknowledge the support of U.S. DOE, NSF, Swiss National Science Foundation, and KOSEF through CSCMR.

*Electronic address: psangior@stanford.edu

[1] E. A. Demler, G. B. Arnold, and M. R. Beasley, Phys. Rev. B **55**, 15174 (1997).
[2] P. Fulde and R. A. Ferrel, Phys. Rev. **135**, A550 (1964).
[3] A. Larkin and Y. Ovchinnikov, Zh. Eksp. Teor. Fiz. **47**, 1136 (1964) [Sov. Phys. JETP **20**, 762 (1965)].
[4] Z. Radovic, M. Ledvij, L. Dobrosavljević-Grujić, A. I. Buzdin, and J. R. Clem, Phys. Rev. B **44**, 759 (1991).
[5] Y. V. Fominov, N. M. Chtchelkatchev, and A. A. Golubov, Phys. Rev. B **66**, 014507 (2002).
[6] A. Buzdin, Phys. Rev. B **62**, 11377 (2000).
[7] M. Zareyan, W. Belzig, and Y. V. Nazarov, Phys. Rev. Lett. **86**, 308 (2001).
[8] A. I. Buzdin, L. N. Bulaevskii, and S. V. Panyukov, Pis'ma Zh. Eksp. Teor. Fiz. **35**, 147 (1982) [JETP Lett. **35**, 178 (1982)].
[9] F. S. Bergeret, A. F. Volkov, and K. B. Efetov, Phys. Rev. Lett. **86**, 4096 (2001).
[10] A. I. Buzdin, Rev. Mod. Phys. **77**, 935 (2005).
[11] K. D. Usadel, Phys. Rev. Lett. **25**, 507 (1970).
[12] H. Doh and H.-Y. Choi, cond-mat/0407149 (unpublished).
[13] V. V. Ryazanov, V. A. Oboznov, A. V. Veretennikov, and A. Y. Rusanov, Phys. Rev. B **65**, 020501(R) (2001).
[14] T. Kontos, M. Aprili, J. Lesueur, F. Genêt, B. Stephanidis, and R. Boursier, Phys. Rev. Lett. **89**, 137007 (2002).
[15] W. Guichard, M. Aprili, O. Bourgeois, T. Kontos, J. Lesueur, and P. Gandit, Phys. Rev. Lett. **90**, 167001 (2003).
[16] C. Strunk, C. Sürgers, U. Paschen, and H. v. Löhneysen, Phys. Rev. B **49**, 4053 (1994).
[17] J. S. Jiang, D. Davidovic, D. H. Reich, and C. L. Chien, Phys. Rev. Lett. **74**, 314 (1995).
[18] T. Mühge, K. Theis-Bröhl, K. Westerholt, H. Zabel, N. N. Garif'yanov, Y. V. Goryunov, I. A. Garifullin, and G. G. Khaliullin, Phys. Rev. B **57**, 5071 (1998).
[19] L. Lazar, K. Westerholt, H. Zabel, L. R. Tagirov, Y. V. Goryunov, N. N. Garif'yanov, and I. A. Garifullin, Phys. Rev. B **61**, 3711 (2000).
[20] J. Aarts, J. M. E. Geers, E. Brück, A. A. Golubov, and R. Coehoorn, Phys. Rev. B **56**, 2779 (1997).
[21] T. Kontos, M. Aprili, J. Lesueur, and X. Grison, Phys. Rev. Lett. **86**, 304 (2001).
[22] T. Kontos, M. Aprili, J. Lesueur, X. Grison, and L. Dumoulin, Phys. Rev. Lett. **93**, 137001 (2004).
[23] L. Crétinon, A. K. Gupta, B. Pannetier, H. Courtois, H. Sellier, and F. Lefloch, Physica C **404**, 110 (2004).
[24] L. Crétinon, A. K. Gupta, H. Sellier, F. Lefloch, M. Fauré, A. Buzdin, and H. Courtois, Phys. Rev. B **72**, 024511 (2005).
[25] O. Bourgeois and R. C. Dynes, Phys. Rev. B **65**, 144503 (2002).
[26] J. Kim, J. H. Kwon, K. Char, H. Doh, and H.-Y. Choi, Phys. Rev. B **72**, 014518 (2005).
[27] E. L. Wolf, *Principles of Electron Tunneling Spectroscopy* (Oxford Science Publications, New York, 1985).
[28] A. J. Heinrich, J. A. Gupta, C. P. Lutz, and D. M. Eigler, Science **306**, 466 (2004).
[29] G. E. Blonder, M. Tinkham, and T. M. Klapwijk, Phys. Rev. B **25**, 4515 (1982).
[30] J. M. MacLaren, T. C. Schulthess, W. W. Butler, R. Sutton, and M. McHenry, J. Appl. Phys. **85**, 4833 (1999).
[31] A. I. Liechtenstein, M. I. Katsnelson, V. P. Antropov, and V. A. Gubanov, J. Magn. Magn. Mater. **67**, 65 (1986).
[32] D. Wang, J. M. Daughton, K. Bussmann, and G. A. Prinz, J. Appl. Phys. **83**, 7034 (1998).
[33] A. C. Reilly, W. Park, R. Slater, B. Ouaglal, R. Loloee, W. P. J. Pratt, and J. Bass, J. Magn. Magn. Mater. **195**, L269 (1998).
[34] K. Halterman and O. T. Valls, Phys. Rev. B **66**, 224516 (2002).
[35] G. Eilenberger, Z. Phys. **214**, 195 (1968).